ELSEVIER

Journal of Nuclear Materials 289 (2001) 263–269

journal of nuclear materials

www.elsevier.nl/locate/jnucmat

The effect of manganese on the strain-induced martensitic transformation and high temperature wear resistance of Fe–20Cr–1C–1Si hardfacing alloy

Jun-ki Kim *, Geun-mo Kim, Seon-jin Kim

Division of Materials Science and Engineering, Hanyang University, 17 Haengdang-dong, Seongdong-gu, Seoul 133-791, South Korea

Received 18 September 2000; accepted 29 December 2000

Abstract

Sliding wear tests of Fe–20Cr–1C–1Si–xMn alloys with x varying from 0 to 25 wt% were performed in air at temperatures of 25–450°C under a contact stress of 103 MPa. During wear at 25°C, low-Mn alloys containing less than 5 wt% Mn and high-Mn alloys containing more than 10 wt% Mn exhibited the $\gamma \rightarrow \alpha'$ and $\gamma \rightarrow \varepsilon$ strain-induced martensitic transformations, respectively. As the test temperature increased, low-Mn alloys showed a wear transition from mild oxidative wear to galling at a temperature between 350°C and 400°C due to the absence of $\gamma \rightarrow \alpha'$ strain-induced martensitic transformation. In the case of high-Mn alloys, the mild oxidative wear was maintained until 450°C, which was the highest test temperature in this study, with the formation of strain-induced ε martensite. It was considered that the $\gamma \rightarrow \varepsilon$ strain-induced martensitic transformation could be more beneficial to the high temperature wear resistance of iron-base hardfacing alloy than the $\gamma \rightarrow \alpha'$ strain-induced martensitic transformation due to the higher M_d temperature. © 2001 Published by Elsevier Science B.V.

1. Introduction

Cobalt-base Stellite™ hardfacing alloys have been used extensively for high temperature applications involving metal–metal wear, abrasive wear, and impact wear, and for erosion and corrosion resistance [1]. However, alternative materials have been sought for many years owing to the high cost of cobalt-base alloys and an increasing reluctance to use cobalt materials for nuclear power applications due to the occupational radiation exposure [2–5].

Galling resistance is of primary importance in the development of a cobalt-free substitute for Stellite because high contact stress, which is a necessary condition for the initiation of galling, is often present in the fields of Stellite usage [4]. Galling is characterized by the severe localized plastic deformation, fracture, and often the transfer of a significant amount of material from one contacting surface to the other [6]. Therefore, the extensive plastic deformation at contacting surfaces should be avoided for galling resistance.

High work hardening rate is desirable for high galling resistance since the highly work hardened surface would resist deformation. It can be achieved by lowering the stacking fault energy (SFE) of materials. The strain-induced martensitic transformation observed in very low SFE materials, such as Stellite alloys, is known to be most beneficial to galling resistance [1,3,7]. The strain-induced martensite formed at the deformed asperity junctions provides an additional ability to fracture, rather than deform [1].

In the case of austenitic iron-base alloys, deformation can result in a martensite that can have either bct or hcp crystal structures, known as α' and ε martensite, respectively [8–11]. The ε martensite is formed from the volume of hcp material produced by the passage of Shockley partial dislocations [9]. The α' martensite can be formed from either the transformation of pre-existing ε martensite [9] or the shear band intersections, such as ε martensites, mechanical twins or stacking faults [8].

* Corresponding author. Tel.: +82-2 2290 0406; fax: +82-2 2293 7844.

E-mail address: alloylab@email.hanyang.ac.kr (J.-k. Kim).

0022-3115/01/$ - see front matter © 2001 Published by Elsevier Science B.V.
PII: S0022-3115(01)00433-0

The $\gamma \rightarrow \alpha'$ strain-induced martensitic transformation has been reported to be an important wear resisting mechanism in an iron-base hardfacing alloy [3,7]. However, the strain-induced α' martensite could be beneficial to the wear resistance only below the M_d temperature [7]. On the contrary, the role of $\gamma \rightarrow \varepsilon$ strain-induced martensitic transformation in the wear resistance of iron-base hardfacing alloys has not been studied extensively.

In this study, the effect of manganese on the strain-induced martensitic transformation behavior of Fe–20Cr–1C–1Si–xMn ($x = 0$–25 wt%) hardfacing alloys was determined, and the role of $\gamma \rightarrow \alpha'$ and $\gamma \rightarrow \varepsilon$ strain-induced martensitic transformations in the high temperature wear resistance of iron-base hardfacing alloys was investigated.

2. Experimental procedure

2.1. Specimen

Small, approximately 30 g, Fe–20Cr–1C–1Si–xMn alloy blocks with x varying from 0 to 25 wt% were arc melted under argon atmosphere using a water-cooled copper crucible and a non-consumable tungsten electrode. The iron used for making alloys was 99.98% pure and the manganese was 99.8% pure. Other alloying elements, such as chromium, silicon and carbon, were added from three master alloys of which chemical composition were Fe–59Cr–0.03C, Fe–58.9Cr–6.36C and Fe–74.2Si. Every block was melted 10 times, and inverted between melting to ensure homogeneity.

The chemical composition of alloys was measured by an ARD 3460 optical emission spectrometer, and their nominal chemical compositions are presented in Table 1. After arc melting, alloy blocks were carefully machined by wire cutting into wear test specimens shown in Fig. 1. The surfaces for wear testing were polished to a roughness value $R_a < 0.02$ μm by grinding with 2000 grit SiC abrasive paper.

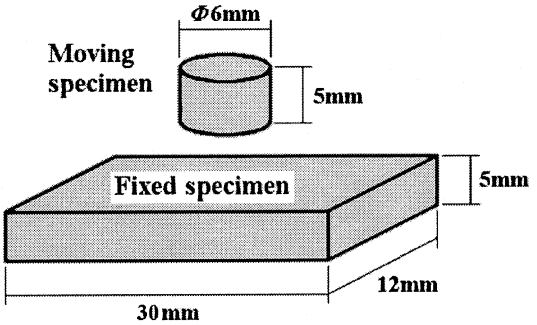

Fig. 1. Geometry of wear test specimens.

2.2. Sliding wear test

The disc-on-plate type reciprocating friction machine manufactured by Plint and Partners was used for these high load sliding wear tests. The wear tests were conducted for self-mated alloys in air at temperatures of 25–450°C. The contact stress, 103 MPa (15 ksi), was chosen from the highest design value of the highly loaded valves [12]. The sliding speed of wear tests was 3 mm/s and the stroke was 9 mm.

The weight changes of the moving and fixed specimens were measured after 100 cycles of sliding except when galling occurred. Galling always occurred at the beginning of the test and the test was stopped immediately. The wear loss of the alloys was represented as the total weight changes of the fixed and moving specimens. More than two replicate tests were performed to obtain reliable data. The relative deviation of the wear loss between tests was below about 10%.

2.3. Examination

The microstructure of alloys were examined from the surface that would be tested. Phase analyses of pre-test specimens were performed by X-ray diffraction (XRD) on the electro-polished surface in order to avoid the strain-induced martensitic transformation during mechanical polishing. The electro-polishing was done in a

Table 1
Nominal chemical composition of specimens (wt%)

Specimen	Element						
	Fe	Cr	C	Si	Mn	P	S
0Mn (Fe–20Cr–1Si–1C)	bal.	19.95	1.004	0.998	–	0.007	0.007
5Mn (Fe–20Cr–1Si–1C–5Mn)	bal.	19.71	0.991	0.986	4.928	0.007	0.009
10Mn (Fe–20Cr–1Si–1C–10Mn)	bal.	19.47	0.979	0.974	9.735	0.007	0.011
15Mn (Fe–20Cr–1Si–1C–15Mn)	bal.	19.23	0.968	0.962	14.43	0.007	0.016
20Mn (Fe–20Cr–1Si–1C–20Mn)	bal.	19.01	0.956	0.950	19.01	0.006	0.014
25Mn (Fe–20Cr–1Si–1C–25Mn)	bal.	18.87	0.945	0.940	23.48	0.006	0.016

solution of methyl alcohol – 10% HCl – 5 g picric acid at 2 V and room temperature.

The worn surface of moving specimens after 100 cycles of sliding and ultrasonic cleaning in acetone were examined by XRD in order to investigate the strain-induced martensites formed during wear. The wear mechanism and the presence of oxide layers were identified from scanning electron microscope (SEM) and wavelength dispersive spectrometer (WDS) analyses. The microstructure of worn surfaces were examined by transmission electron microscope (TEM) to confirm the strain-induced martensitic transformation. TEM specimens were prepared by electro-polishing technique in a solution of acetic acid – 10% perchloric acid at 10 V and −70°C.

3. Results and discussion

3.1. Microstructure

XRD patterns of Fe–20Cr–1C–1Si–*x*Mn alloys obtained from electro-polished surfaces are presented in Fig. 2. The alloys containing 0–25 wt% Mn were fully austenitic and Cr_7C_3 type carbides were formed. The microstructure of the alloys were the typical hypo-eutectic structure as shown in Fig. 3. The amount of eutectic carbides was about 23–25 vol.%. As the manganese content increased, the dendritic structure seemed to be obscured but the type and the amount of carbides were not changed.

3.2. Wear behavior at 25°C

The wear loss of all alloys after 100 cycles of sliding at 25°C under 103 MPa was less than 0.4 mg which is considered negligible. The wear scar shown in Fig. 4 for the case of 5Mn alloy indicates that mild, adhesive wear was dominant at 25°C. XRD patterns obtained from the worn surfaces of moving specimens tested at 25°C are presented in Fig. 5. At the worn surface of alloys containing less than 5 wt% Mn, the α′ martensite was observed. On the contrary, ε martensite was found at the worn surface of alloys containing more than 10 wt% Mn. Although the presence of ε martensite was hard to be observed from XRD patterns shown in Fig. 5, it could be confirmed from TEM observations, as shown in Fig. 12.

It is a well known phenomenon in austenitic iron- and cobalt-base alloys having very low stacking fault energies that martensite can be formed by strain-induced martensitic transformation during plastic deformation; the fcc → hcp strain-induced martensitic transformation in Stellite alloys [1], and both γ → α′ and γ → ε strain-induced martensitic transformations in austenitic iron-base alloys [8–11]. In the case of Fe–20Cr–1C–1Si–*x*Mn alloys, the γ → α′ strain-induced martensitic transformation was predominant at the low manganese content but the addition of manganese above 10 wt% seemed to promote the formation of strain-induced ε martensite.

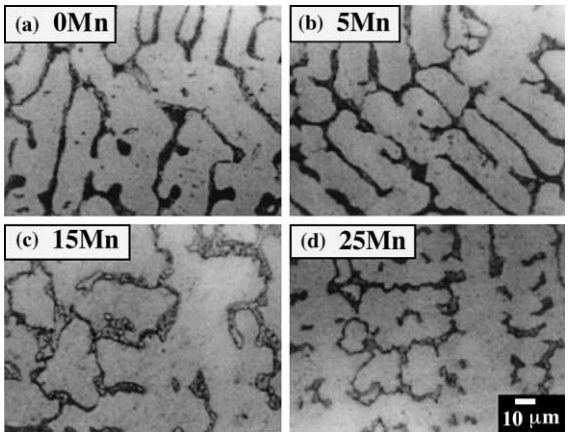

Fig. 3. Optical microstructure of Fe–20Cr–1Si–1C–*x*Mn alloys.

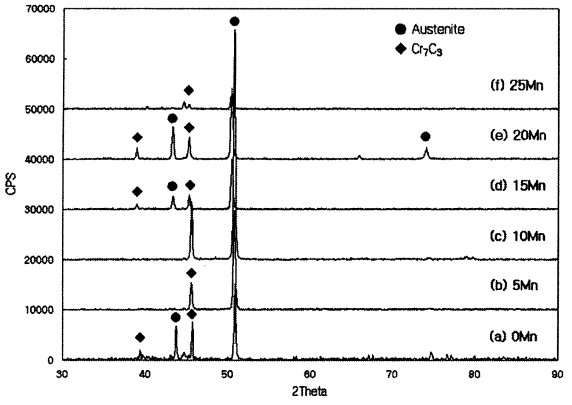

Fig. 2. XRD patterns of Fe–20Cr–1Si–1C–*x*Mn alloys obtained from the electro-polished surface.

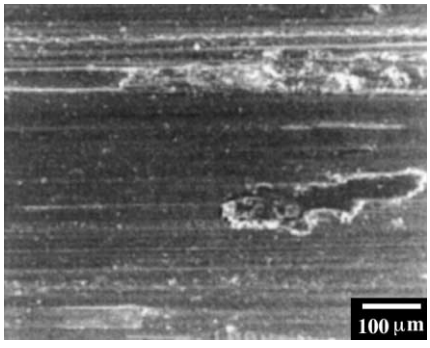

Fig. 4. SEM micrograph of the worn surface of 5Mn alloy tested at 25°C.

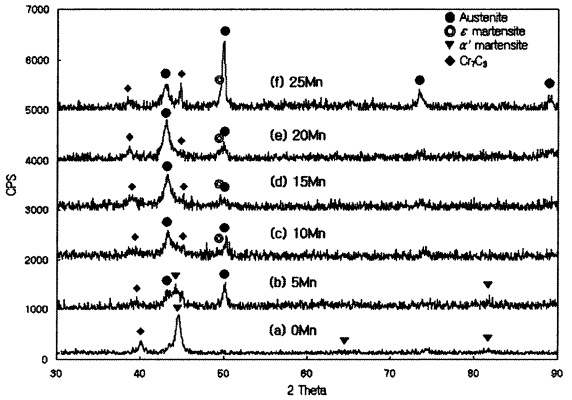

Fig. 5. XRD patterns of worn surfaces of Fe–20Cr–1Si–1C–*x*Mn alloys tested at 25°C.

3.3. High temperature wear of low-Mn alloys

A low-Mn alloy was defined here as an alloy containing less than 5 wt% Mn which formed the strain-induced α′ martensite during wear at 25°C. The wear loss of 0Mn and 5Mn alloys as a function of temperature are presented in Fig. 6. As the temperature increased from 25°C, the amount of wear loss increased until 250°C. After a significant drop of wear loss at 300°C, the wear loss increased again and galling occurred above 400°C for both 0Mn and 5Mn alloys. This indicates that 0Mn and 5Mn alloys lost their wear resistance at a temperature between 350°C and 400°C.

SEM micrographs of the worn surfaces of 5Mn alloy tested at various temperatures are shown in Fig. 7. The wear mechanism changed with temperature: adhesive wear at 250°C, oxidative wear at 350°C and galling at 450°C. It is a well known phenomenon in some iron- and nickel-base alloys that oxidative wear can take place at temperatures of about 200°C or higher due to the formation of wear protective oxide layers [13,14]. These oxide layers formed on contacting surfaces reduce the amount of wear loss by reducing the possibility of direct metal-to-metal contact. There is no doubt that the significant decrease in wear loss at 300°C is owed to a change of dominant wear mechanism from adhesive to oxidative wear.

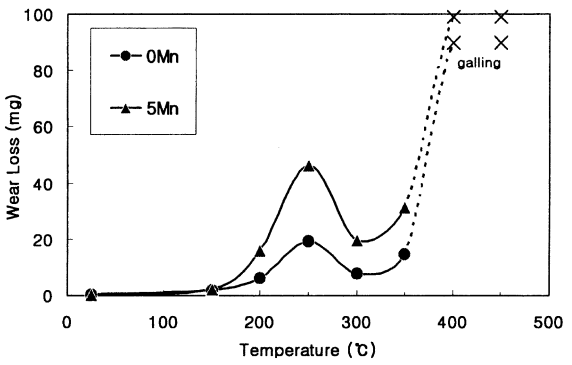

Fig. 6. The wear loss of 0Mn and 5Mn alloys as a function of temperature after 100 cycles of sliding under 103 MPa.

Although higher temperatures are more favorable for oxidative wear due to the accelerated oxidation rate, no oxide layer was found at the worn surface tested at 450°C, as shown in Fig. 7(c). This result can be understood from the formation mechanism of oxide layers. According to Jiang et al. [13], oxide layers leading to the oxidative wear are formed from the compaction of agglomerated small oxidized debris particles on the rubbing surfaces. If there were no chance to generate small debris particles or to be compacted on the rubbing surfaces, the oxidative wear would be made unlikely, even at high temperatures. Instead, the softening of the subsurface material, which leads to the severe plastic deformation, would overwhelm oxidational effects on wear.

The topography of the surface damage observed in Fig. 7(c) has been referred to as prow which indicates the occurrence of galling [6]. Galling occurs when the local contact stresses are sufficiently large that shear deformation extends deep into the contacting surfaces resulting in the gross plastic deformation and fracture [15]. The wear transition from mild oxidative wear to galling at a temperature between 350°C and 400°C indicates that the resistance to plastic deformation was significantly reduced at the corresponding temperature.

XRD patterns obtained from the worn surfaces of 5Mn alloy tested at various temperatures are presented in Fig. 8. The α′ martensite could be found at the worn surfaces tested below 350°C but it did not observe any more at 400°C. This could be confirmed by TEM observations shown in Fig. 9. At the worn surface of 5Mn alloy tested at 25°C, platelets of strain-induced α′ martensite were found (see Fig. 9(a)). However, only tangled dislocations could be found at the worn surface tested at 450°C (Fig. 9(b)).

The M_d temperature is defined as the maximum temperature at which the strain-induced martensitic transformation can take place during deformation [8]. These observations indicate that the M_d temperature of $\gamma \rightarrow \alpha'$ strain-induced phase transformation in 5Mn alloy was located between 350°C and 400°C. This M_d temperature was consistent with the wear transition temperature from mild oxidative wear to galling. It has been reported that the M_d temperature determines the temperature limit of wear resistance by affecting the work hardening rate in an iron-base hardfacing alloy which showed the $\gamma \rightarrow \alpha'$ strain-induced martensitic transformation during wear [7].

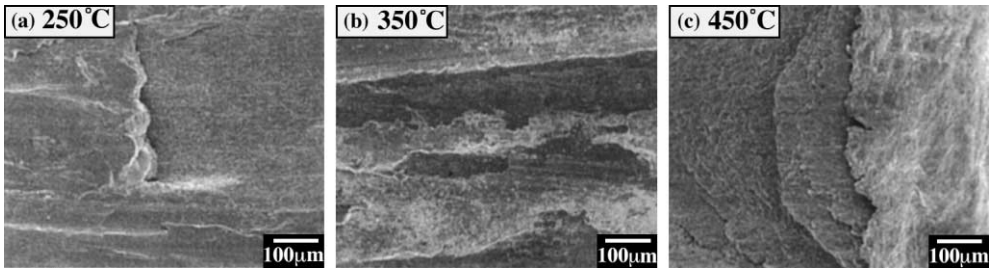

Fig. 7. SEM micrographs of worn surfaces of 5Mn alloy tested at various temperatures.

There was no significant difference between 0Mn and 5Mn alloys in terms of their high temperature wear behavior, as shown in Fig. 6, except that 5Mn alloy showed somewhat larger amount of wear loss than 0Mn alloy. Therefore, it was considered that the small addition of manganese by less than 5 wt% hardly changed the M_d temperature of $\gamma \rightarrow \alpha'$ strain-induced martensitic transformation in Fe–20Cr–1C–1Si alloy but it seemed to be detrimental to the high temperature wear resistance in the viewpoint of wear loss.

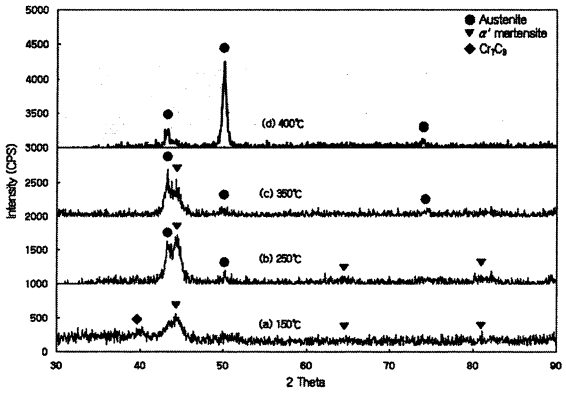

Fig. 8. XRD patterns of worn surfaces of 5Mn alloy tested at various temperatures.

3.4. High temperature wear of high-Mn alloys

A high-Mn alloy was defined here as an alloy containing more than 10 wt% Mn which formed strain-induced ε martensite during wear at 25°C. The wear loss of 10Mn, 15Mn, 20Mn and 25Mn alloys as a function of temperature are presented in Fig. 10. Similar to the case of low-Mn alloys shown in Fig. 6, the wear loss of high-Mn alloys increased with temperature until 250°C and there was a decrease in wear loss at 300°C. However, high-Mn alloys maintained decreased wear losses until 450°C, which was the highest test temperature in this study, while low-Mn alloys showed galling above 400° C.

SEM micrographs of the worn surfaces of 15Mn alloy tested at various temperatures were shown in Fig. 11. It was observed that the dominant wear mechanism at 250°C was the adhesive wear but that oxidative wear was dominant at 350°C and 450°C. It was obvious that the low wear loss of high-Mn alloys at high temperature up to 450°C was due to their ability to maintain the

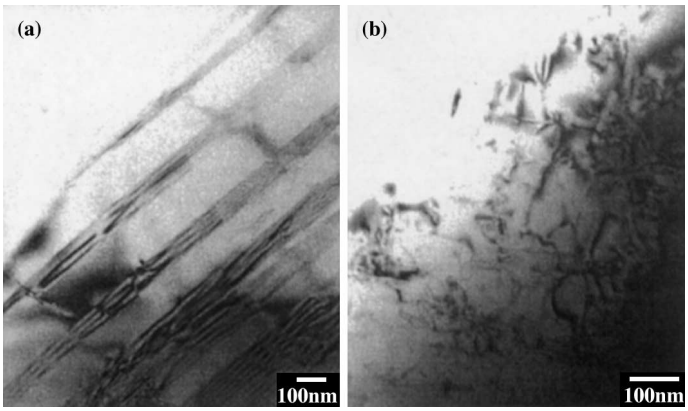

Fig. 9. TEM micrographs of worn surfaces of 5Mn alloy; (a) tested at 25°C and (b) tested at 450°C.

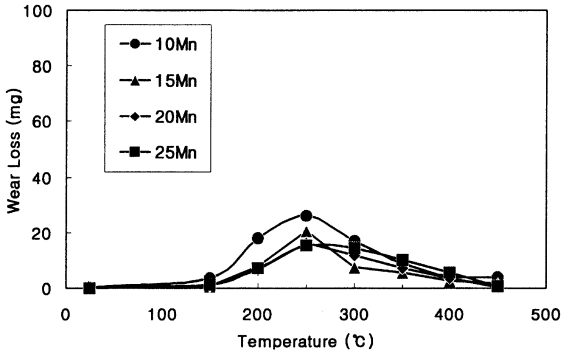

Fig. 10. The wear loss of 10Mn, 15Mn, 20Mn and 25Mn alloys as a function of temperature after 100 cycles of sliding under 103 MPa.

oxidative wear. This indicates that there was no significant loss of their resistance to severe plastic deformation causing galling. The existence of strain-induced ε martensite at the worn surface of 15Mn alloy tested at 450°C could be confirmed from TEM observations like that shown in Fig. 12. Therefore, it was concluded that the M_d temperature of $\gamma \rightarrow \varepsilon$ strain-induced martensitic transformation in high-Mn alloys was higher than 450°C.

It is well known that the strain-induced α' martensite is formed from shear band intersections, such as stacking faults, twins, and ε martensite platelets [8]. According to Olson and Cohen [16], the amount of strain-induced α' martensite is reduced with increasing temperature because the formation of shear bands, the possibility of their intersections and the probability that an embryo of α' martensite can be created at the shear band intersections are decreased. Unlike the strain-induced α' martensite, the strain-induced ε martensite is known to be formed by the simple mechanism, the passage of partial dislocations [9]. This means that the $\gamma \rightarrow \varepsilon$ strain-induced martensitic transformation can be operative at higher temperature than the $\gamma \rightarrow \alpha'$ strain-induced martensitic transformation. Therefore, it was considered that the $\gamma \rightarrow \varepsilon$ strain-induced martensitic transformation would be more beneficial due to the high temperature wear resistance of iron-base hardfacing alloys than the $\gamma \rightarrow \alpha$ strain-induced martensitic transformation due to the higher M_d temperature.

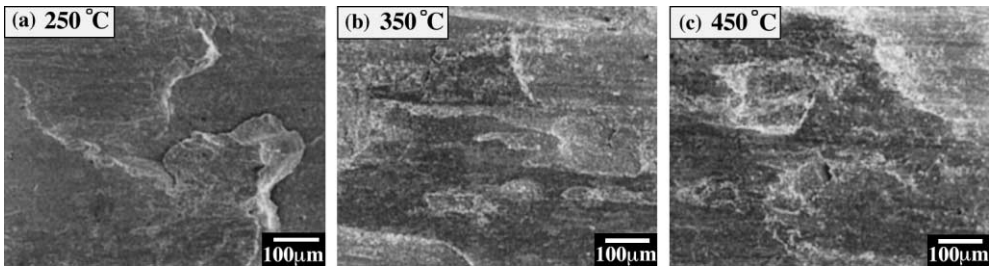

Fig. 11. SEM micrographs of worn surfaces of 5Mn alloy tested at various temperatures.

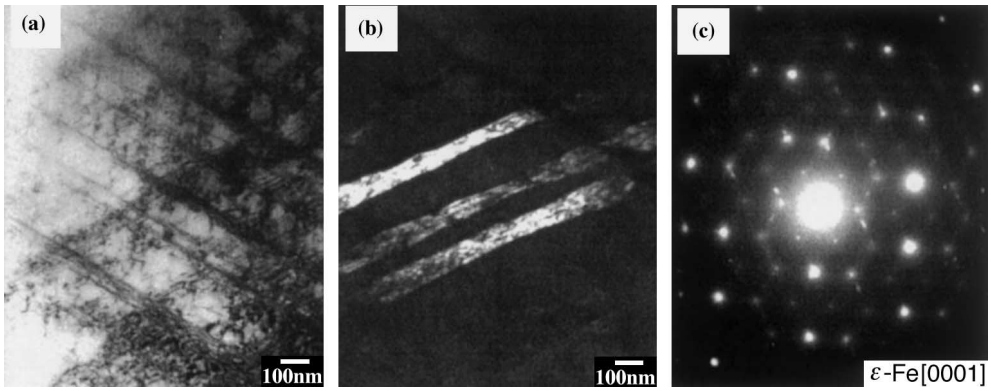

Fig. 12. TEM micrographs of the worn surface of 15Mn alloy tested at 450°C: (a) bright field image, (b) dark field image and (c) SAD pattern corresponding to (b).

4. Conclusions

From sliding wear tests of Fe–20Cr–1C–1Si–xMn ($x = 0$–25 wt%) alloys in air at temperatures of 25–450°C under a contact stress of 103 MPa, the following conclusions could be achieved.

1. Additions of manganese of less than 5 wt% did not affect the high temperature wear behavior of Fe–20Cr–1C–1Si alloy. It was considered that the M_d temperature of $\gamma \rightarrow \alpha'$ strain-induced martensitic transformation was hardly changed.
2. Additions of manganese exceeding 10 wt% improved the high temperature wear resistance of the Fe–20Cr–1C–1Si alloy. It was considered to be due to the development of $\gamma \rightarrow \varepsilon$ strain-induced martensitic transformation.
3. The $\gamma \rightarrow \varepsilon$ strain-induced martensitic transformation is considered to be more beneficial to the high temperature wear resistance of iron-base hardfacing alloys than the $\gamma \rightarrow \alpha'$ strain-induced martensitic transformation owing to the higher M_d temperature.

Acknowledgements

This work was supported by the Korea Science and Engineering Foundation (KOSEF) through the Innovative Technology Center for Radiation Safety (iTRS), Hanyang University, South Korea.

References

[1] K.C. Antony, J. Met. (1983) 52.
[2] H. Ocken, Nucl. Technol. 68 (1985) 18.
[3] E.K. Ohriner, T. Wada, E.P. Whelan, H. Ocken, Metall. Trans. A 22 (1991) 983.
[4] J. Vikstrom, Wear 179 (1994) 143.
[5] H. Ocken, Surf. Coating Tech. 76&77 (1995) 456.
[6] L.K. Ives, M.B. Peterson, E.P. Whitenton, in: F.A. Smlidt, P.J. Blau (Eds.), Proceedings of Engineered Materials for Advanced Friction and Wear Applications, Gaithersburg, MD, USA, 1–3 March 1988, p. 33.
[7] J.K. Kim, S.J. Kim, Wear 237 (2000) 217.
[8] F. Lecroisey, A. Pineau, Metall. Trans. 3 (1972) 387.
[9] J.W. Brooks, M.H. Loretto, R.E. Smallman, Acta Metall. 27 (1979) 1839.
[10] K.L. Hsu, T.M. Ahn, D.A. Rigney, Wear 60 (1980) 13.
[11] Z. Fucheng, L. Tingquan, Wear 212 (1997) 195.
[12] H. Ocken, Cobalt reduction guidelines, Rep. EPRI NP-6737, Electric Power Research Institute, March 1990.
[13] J. Jiang, F.H. Scott, M.M. Stack, Wear 176 (1994) 185.
[14] H. So, Wear 184 (1995) 161.
[15] K.J. Bhansali, A.E. Miller, Wear 75 (1982) 241.
[16] G.B. Olson, M. Cohen, Metall. Trans. A 6 (1975) 791.